J Mol Model (2012) 18:2717–2725
DOI 10.1007/s00894-011-1295-x

ORIGINAL PAPER

# Exploration of conformational transition in the aryl-binding site of human FXa using molecular dynamics simulations

**Jing-Fang Wang · Pei Hao · Yi-Xue Li · Jian-Liang Dai · Xuan Li**

Received: 19 October 2010 / Accepted: 24 October 2011 / Published online: 25 November 2011


**Abstract** Human coagulation Factor X (FX), a member of the vitamin K-dependent serine protease family, is a crucial component of the human coagulation cascade. Activated FX (FXa) participates in forming the prothrombinase complex on activated platelets to convert prothrombin to thrombin in coagulation reactions. In the current study, 30-ns MD simulations were performed on both the open and closed states of human FXa. Root mean squares (RMS) fluctuations showed that structural fluctuations concentrated on the loop regions of FXa, and the presence of a ligand in the closed system resulted in larger fluctuations of the gating residues. The open system had a gating distance from 9.23 to 11.33 Å, i.e., significantly larger than that of the closed system (4.69–6.35 Å), which allows diversified substrates of variable size to enter. Although the solvent accessible surface areas (SASA) of FXa remained the same in both systems, the open system generally had a larger total SASA or hydrophobic SASA (or both) for residues surrounding the S4 pocket. Additionally, more hydrogen bonds were formed in the closed state than in the open state of FXa, which is believed to play a significant role in maintaining the closed confirmation of the aryl-binding site. Based on the results of MD simulations, we propose that an induced-fit mechanism governs the functioning of human coagulation FX, which helps provide a better understanding of the interactions between FXa and its substrate, and the mechanism of the conformational changes involved in human coagulation.

**Keywords** Human coagulation Factor X · Serine-protease domain · Structural transition · Molecular dynamics simulation

J.-F. Wang · Y.-X. Li
Key Laboratory of Systems Biomedicine (Ministry of Education), Shanghai Center for Systems Biomedicine, Shanghai Jiaotong University, Shanghai 200240, China

P. Hao · X. Li
Institute of Plant Physiology and Ecology, Shanghai Institutes for Biological Sciences, Chinese Academy of Sciences, Shanghai 200031, China

P. Hao
e-mail: phao@sibs.ac.cn

X. Li
e-mail: lixuan@sippe.ac.cn

J.-F. Wang (✉) · P. Hao · Y.-X. Li · X. Li
Shanghai Center for Bioinformation Technology, Shanghai 200235, China
e-mail: jfwang8113@gmail.com

J.-F. Wang · J.-L. Dai
School of Life Sciences, Fudan University, Shanghai 200433, China

J.-L. Dai
e-mail: jldai@scbit.org

## Introduction

Human coagulation factor X (FX) is a vitamin K-dependent serine protease that plays a critical role in the activation and regulation of the blood coagulation cascade [1]. As a central factor in the coagulation process, FX is activated and regulated by a series of events. FX is synthesized in the liver and released into the circulation in the zymogenic form. Zymogenic FX is activated by multiple proteolytic events, catalyzed either by factor VIIa-tissue factor complex (extrinsic tenase) or factor Ixa-VIIa complex (Intrinsic tenase). Activated FX (FXa) then interacts with factor Va on the phospholipid surface to form the prothrombinase complex. In the presence of calcium ions, this complex

activates prothrombin to thrombin, which in turn converts fibrinogen to fibrin [2]. The blood coagulation cascade is strictly controlled and regulated, and a number of thrombotic or bleeding disorders due to mutated or defective coagulation factors have been reported, including hemophilia, myocardial infarction, von Willebrand disease [3–5] and Stuart-Prower factor deficiency [6, 7].

FXa contains a serine-protease domain of 254 amino acids (Fig. 1), which consists of the active site catalytic triad of His-57, Asp-102, and Ser-195, and two major interaction pockets: the S1 specificity site and the S4 aryl-binding site. Substrate binding to the S1 site involves the formation of a salt-bridge with Asp-189 at the bottom of the pocket, which is surrounded by hydrophobic walls [8, 9]. The S4 site is created on three sides by residues Tyr-99, Phe-174, and Trp-215, which form a hydrophobic sleeve that allows residues like isoleucine, glutamate and proline of substrates to bind [10–13].

FXa recognizes substrates with some variable sequences at their cleavage site [14]. The structure of FXa and its interactions with substrates have been the subject of intense study over the past two decades. Since the first crystal structure of FXa was published in 1993 [15], a total of more than 50 X-ray crystal structure studies of FXa have been defined. In analyzing the data obtained from X-ray crystal structures of FXa, Singh and Briggs [16] proposed a hypothesis of conformational diversity of FXa that differs from the common "induced fit" enzyme–substrate interaction model. In their hypothesis, to explain the interaction between the binding sites of FXa and its various substrates, they suggested that a substrate "locks" into one good-fit conformation from many different conformations that exist transiently, and that the substrate specificity is determined by the conformational diversity of FXa.

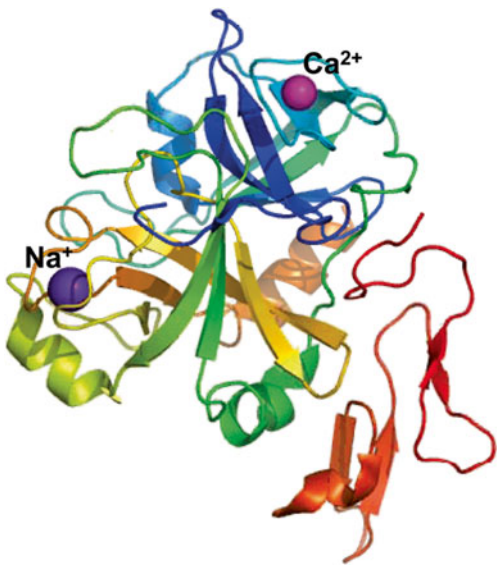


**Fig. 1** Illustration of the three-dimensional structure of activated Factor X (FXa). Only the backbone atoms of FXa are shown in the cartoon representation, and sodium and calcium ions are colored *magenta* and *pink*, respectively

In comparison with the X-ray crystal structure studies of FXa, molecular dynamics (MD) simulation has the advantage of being able to analyze the conformational fluctuations of the FXa molecule and the dynamics of the transient states of FXa. MD simulation on FXa can complement X-ray crystal structure studies in obtaining information on the mobility and flexibility of FXa active-site residues, the solvation of the active-site, and the location of water molecules in the active site. Thus, MD simulations have been used widely to solve problems in protein structural analysis [17–27] and rational drug design [28–37]. MD simulation was performed previously on FXa by Daura et al. [38] and Venkateswarlu [39]. Due to the limitation of computing power at the time those studies were performed, their longest simulation times were 1.5 and 6.2 ns, respectively, which were not adequate to reveal the complete details of the conformational transitions of FXa. More recently, Singh and Briggs [16] adopted a steered MD method to simulate the transition process of human FXa in the S4 site. They used the FXa structure (pdb code 1p0s) bound with ecotin, which they believe represents a closed state of the S4 site. They applied an external force on the backbone of the ecotin molecule during their simulations.

There are currently 53 crystal structures of FXa in the PDB database at Brookhaven. We have surveyed all the available structures of FXa and chosen PDB entries 1c5m [12] and 3cen [40] for our MD simulations. In this paper, we present the results from 30-ns MD simulations performed on both the open and closed forms of FXa. In order to reveal the conformational transition in the serine-protease domain and its aryl-binding site we also present the root mean square (RMS) deviations and fluctuations for Cα atoms that were computed from these simulations. Based on the simulation results, we further discuss the mechanism governing the functioning of human coagulation FX.

## Computational methods

### Generation of the initial models of FXa

In order to generate the initial models for MD simulations, we investigated the available structures from PDB, and chose PDB entry 1c5m [12] for the open system and 3cen [40] as the closed system. 1c5m is unique among all the FXa structures in that it contains no ligand and has the largest S4 pocket size [distance between the gating residues (Tyr-99 and Phe-174)>10 Å)] and hence represents the open state of FXa. 3cen—234 residues—contains a small

molecular ligand Anthranilamide 28 (N-(2-(((5-chloro-2-pyridinyl)amino)sulfonyl)phenyl)-4-(2-oxo-1(2H)-pyridinyl) benzamide) and is resolved to 2.80 Å. It has one of the smallest S4 pockets [distance between the gating residues (Tyr-99 and Phe-174) ~8 Å] among all available FXa structures, and thus represents the closed state of FXa. Both crystal structures were obtained from the PDB database at Brookhaven [41], and MD simulations were performed on the serine protease domain. Although substantial experimental evidence shows that ions bound close to the serine protease domain (as shown in Fig. 1) crucially influence the function of FXa, to maintain the starting structure we did not involve these ions originally in our simulations [42, 43]. The full sequences from the original PDB models were used in order to keep the integrity of their molecular structure. The sequences of FXa used as open and closed systems (16–251 for the open system and 16–244 for the closed system) cover the entire active binding sites of the serine protease domain. In addition to the open and closed systems, we also added a system of the closed structure with the ligand deleted. The initial structures of this system were selected randomly from the simulation trajectories of the closed structure.

### Molecular dynamics simulations

MD simulations on the initial models of both the open and closed systems were performed under the periodic boundary conditions using the software GROMACS (Version 3.3.3) [44] with GROMOS96 force field parameters [45]. The topology files, charges, and force field parameters of the ligand atoms for the closed system of FXa were re-generated using the online software PRODRG [46], and further confirmed by quantum chemistry (QM) calculations at DFT-B3LYP using the Gaussian03 program. As the closed system has a ligand comprising a halogen–π interaction in the closed system, which is believed to contribute crucially to the interaction energy of the protein, the force field may be not able to accurately describe this interaction [47, 48]. However, since the aim of the present study was to detect structural differences in the protein with and without ligand binding, our simulations focus mainly on the protein. As a result, the loose description of the halogen–π interaction has little influence in our simulations. Before the simulations started, both systems were put into the explicit SPC water boxes with a depth of 1.0 nanometers (nm) from the surface of the FXa molecule. To neutralize redundant charges in the system, 13 and 14 chlorine ions were added to the open and closed systems at pH 7.0, respectively, by replacing an equal number of solvent waters in both systems.

During MD simulations, all bonds were constrained by the LINear Constraint Solver (LINCS) algorithm and atoms velocities for start-up runs were obtained according to the Maxwell distribution at 310 K. The temperature of FXa, solvent and ligand were coupled separately, through a Berendsen thermostat, to a bath at temperature 310 K with a time constant of 0.1 ps. Isotropic pressure coupling of both systems was based on the Berendsen weak coupling algorithm with time constant 1.0 ps and compressibility of $4.5\times10^{-5}$ per bar. Subsequently, the neutralized systems were subjected to energy minimization with the steepest descent method to a maximum gradient of 2,000 kJ $mol^{-1}$ $nm^{-1}$. A constant pressure of 1 bar was applied independently in the X, Y, and Z directions. Short MD simulations (about 1 ns) were performed for both systems with all FXa and ligand atoms fixed to reduce the van der Waals conflicts. The electrostatic interactions were calculated by the PME algorithm with an interpolation order of 4 and a grid spacing of 0.12 nm. In addition, the van der Waals interactions were calculated using a cut-off of 12 Å. The solvent accessible surface area (SASA) involved in our study was computed using the linear combinations of pairwise overlaps (LCPO) approach. A total of 30-ns of MD simulations were performed with a time step of 2 fs, and coordinates for all atoms in both systems were saved every 1 ps.

## Results and discussion

### Global properties

The average energies of both the open and closed systems were relatively constant throughout the simulation processes, indicating that both systems have reached their equilibrium states in our MD simulations. The total energies fluctuated an approximate value of $-2.90\times10^{5}$ kJ $mol^{-1}$ for the open system and $-2.97\times10^{5}$ kJ $mol^{-1}$ for the closed system, respectively. RMS deviation from the initial models is an important criterion with which to assess the convergence of protein systems. As shown in Fig. 2a, the RMS deviation values of Cα atoms (calculated from the starting structure) were 3.06±0.429 Å for the open system and 3.16±0.636 Å for the closed system. The open system reached its equilibrium state after about 800 ps, while the closed system did it in about 500 ps.

To give a detailed picture of the conformational sampling for all the simulated systems, we also computed 2D RMS deviation values for the backbone structure of FXa, considering the mutual RMS deviation distances among all snapshots along the simulation trajectories (Fig. 3). The 2D RMS deviation results also support the fact that both open and closed systems are in equilibrium. However, unlike the 1D RMS deviations, 2D RMS deviation analysis gave an indication that some conformational transitions occurred during MD simulations (giving comparatively high RMS deviation values). Interestingly, the RMS deviation value for the closed system without any ligand in the active site

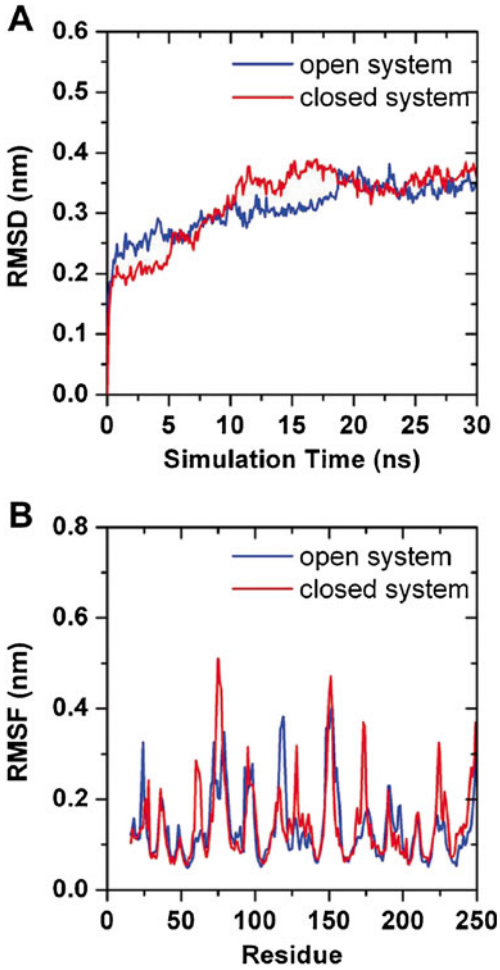


**Fig. 2** Trajectory analyses of 30-ns molecular dynamics (MD) simulations. **a** Time-dependent root mean square (RMS) deviations of Cα atoms, and **b** RMS fluctuations of Cα atoms. The *blue* and *red curves* represent the open and closed systems, respectively

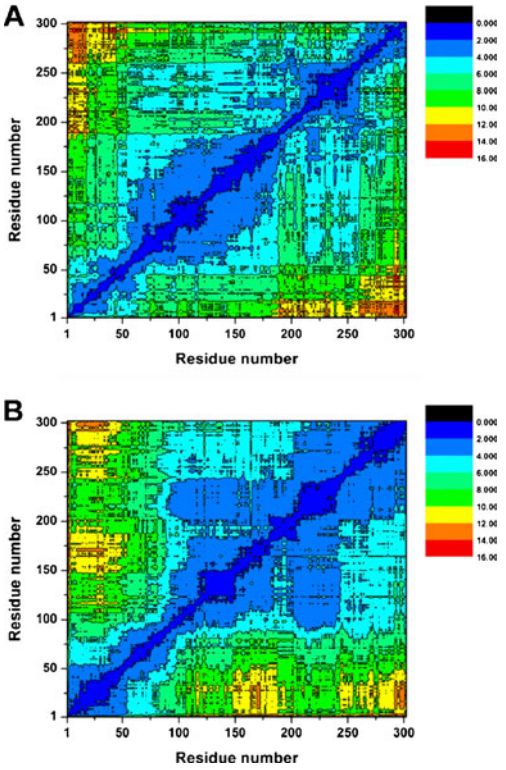


**Fig. 3** 2D RMS deviation plots for the backbone structures of **a** open and **b** closed systems. The RMS deviation values (Å) are colored from *black* (RMS deviation = 0) to *red* (RMS deviation = 16 Å)

was ~3.13 Å after a 6-ns simulation. As the RMS deviation values are very similar, we calculated the radius of gyration for Cα atoms to estimate the size of proteins in both systems.

The radius of gyration for the open system (1.60± 0.01 nm) was larger than that of the closed system (1.58± 0.01 nm). As the radius of gyration of an object describes its dimensions, calculated as the root mean square distance (RMSD) between its center of gravity and its ends, this value in the protein structure is indicative of the level of compaction in the structure, i.e., how folded or unfolded the protein is. The difference in the radius of gyration for the open and closed systems is quite small, revealing that the structural differences between the open and closed systems are caused mainly by structural motion rather than protein folding. We further computed the RMS fluctuations for residues in both systems. As shown in Fig. 2b, the main difference in RMS fluctuations for both systems exists in residues 55–75, 90–100, 110–130, 165–180, and 225–230. These residues are located mainly on the loop regions and are gating residues of the aryl-binding site.

As a globular enzyme with a very high water concentration, the dynamic behavior of FXa is believed to be influenced by water molecules nearby. For proteins with a serine protease domain, a total of 21 conserved water binding sites have been identified to date [49–51]. Wallnoefer et al. [52] present a clustering approach to generate a representative intraprotein water network for human FXa based on the structural information available for the protein. They found that water molecules have a significant influence on the global properties of the dynamic behavior of human FXa, which reflects the stabilization and flexibility of the proteins. The binding pocket especially is extremely sensitive to the position of water molecules.

## Conformational transitions in the aryl-binding site

The aryl-binding site is a pocket created by residues Tyr-99, Phe-174, and Trp-215 on three sides as displayed in Fig. 4. To determine the flexibility of these residues, we calculated their RMS deviations and fluctuations from the 30-ns MD simulations. The average RMS deviation values for the Cα atoms of Tyr-99 were 1.24±0.24 Å for the open system and 0.55±0.19 Å for the closed system, with a difference of

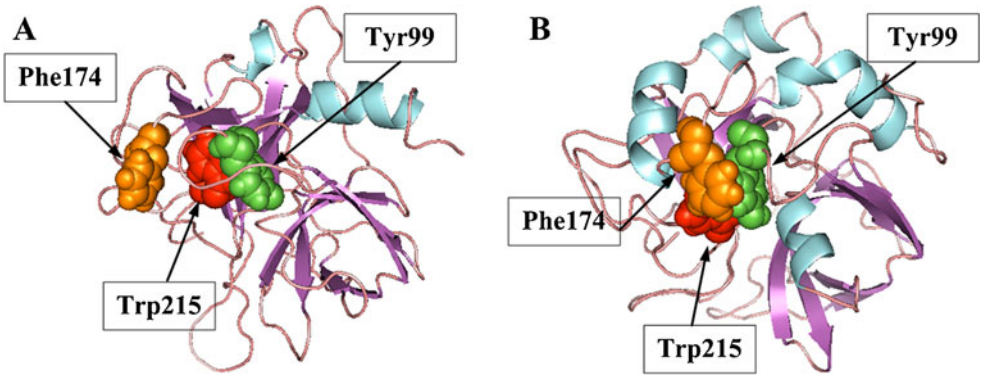


**Fig. 4** Conformation of the gating residues in the open and closed states of FXa. The figure was produced using program PyMol 0.99 to illustrate the residues Tyr-99 (*green*), Phe-174 (*orange*), and Trp-215 (*red*) in the aryl-binding site for the open state (**a**), and the closed state (**b**)

0.69 Å. However, the RMS fluctuation value of Tyr-99 for the closed system was almost 50% higher than that of the open system (0.18 vs 0.12), suggesting that this residue is more flexible in the closed system. The RMS deviation values for the Cα atoms of Phe-174 had larger fluctuations for both systems (0.77±0.48 Å and 0.92±0.45 Å for the open and closed system, respectively), indicating that this residue exhibits conformational diversity in both systems. Unlike Tyr-99 and Phe-174, the RMS deviation values for the Cα atoms of Trp-215 were almost the same for both systems in 0–13 ns simulations (Fig. 5a). However, large fluctuations appeared in 13–30 ns simulations. Because residues Tyr-99 and Phe-174 stand on opposite sides of the S4 pocket, which controls the size of the aryl-binding site, we define the distance between them as the "gating distance" (Fig. 5b). The open system had a gating distance of 9.23–11.33 Å, i.e., significantly larger than that of the closed system: 4.69–6.35 Å. Because of its larger gating distance, the open system allows diverse substrates with variable size to enter. This is also supported by experimental data showing that FXa can adopt substrates with various sequences at the P4/P4′ site. As shown in Table 1, the sizes of the P4/P4′ residues (P4 is the fourth amino acid upstream of the scissile bond, P4′ is the fourth amino acid downstream) appear to be a good fit for the aryl-binding pocket in the open system of FXa. We also performed MD simulations on the closed system with the ligand deleted. After 6-ns simulation, the gating distance (4.70 Å in the starting structure) became 10.65 Å, revealing that, without ligand binding, FXa in the closed conformation changed its structure to an open conformation.

Different gating distances can cause changes in the solvent accessible surface area (SASA) in the aryl-binding site of the open and closed systems of FXa. The hydrophobic SASA was defined as the SASA contributed by the hydrophobic components of the residue [53–55]. As shown in Table 2, while the hydrophobic and total SASA of the entire FXa molecule remained the same between both the open and closed system, the open system generally produced larger total SASA or hydrophobic SASA (or both) for the residues surrounding S4 pocket: His-57, Tyr-99, Asp-102, Asp-189, Ser-195, and Trp-215, with the exception of Phe-174. These data suggest different

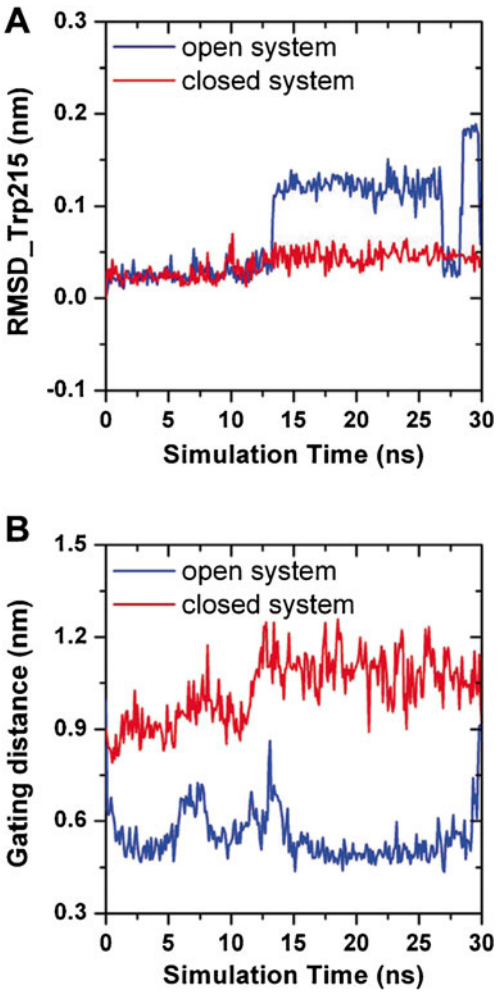


**Fig. 5** Structural variation in the gating residues of FXa. **a** RMS deviations of Trp-215 plotted between 0 and 30 ns for both the open (*blue line*) and the closed (*red line*) systems. The gating distances of aryl-binding site defined by Tyr-00 and Phe-174 are illustrated in (**b**) with the open and closed systems being colored in *blue* and *red*, respectively

**Table 1** Sequences of various FXa substrates that are near their cleavage sites. The size of each amino acid residue calculated from the side chain length is included in the bracket next to each residue

| | Prothrombin | Meizothrombin | Factor VII | Autocatalytic loop |
|---|---|---|---|---|
| P4[a] | I (4.71 Å) | P (3.33 Å) | I (4.71 Å) | E (5.65 Å) |
| P3 | D (4.25 Å) | Q (3.74 Å) | E (5.65 Å) | K (6.43 Å) |
| P2 | G (2.44 Å) | G (2.44 Å) | G (2.44 Å) | G (2.44 Å) |
| P1 | R (7.32 Å) | R (7.32 Å) | R (7.32 Å) | R (7.32 Å) |
| P1′ | I (4.71 Å) | I (4.71 Å) | T (2.44 Å) | Q (3.74 Å) |
| P2′ | V (3.94 Å) | V (3.94 Å) | A (1.53 Å) | S (2.47 Å) |
| P3′ | E (5.65 Å) | G (2.44 Å) | T (2.44 Å) | T (2.44 Å) |
| P4′ | G (2.44 Å) | G (2.44 Å) | S (2.47 Å) | R (7.32 Å) |

[a] P1, P2, P3, and P4 are the first, second, third, and fourth amino acids upstream of the scissile bond, and P1′, P2′, P3′, and P4′ are the first, second, third, and fourth amino acids downstream

structural environments for these residues between the open and the closed states of FXa. In addition, the gating residue Tyr-99 is more exposed in the open system than in the closed system, whereas Phe-174 is more exposed in the closed system than in the open system.

Hydrogen bonds are the key factor in maintaining the 3D structure of proteins. They are also involved in interactions between enzymes and their substrates. In this study, to determine if hydrogen bonds are involved in forming the spatial confirmation of FXa, we analyzed the hydrogen bonds formed by the gating residues. Two geometrical criteria were used in defining a hydrogen bond in this study: (1) the distance between donor and acceptor is within 0.35 nm; and (2) the angle between hydrogen atom, donor and acceptor is within 30°. A number of intra-molecular hydrogen bonds formed by the gating residues were detected, and are listed in Table 3. In general, fewer hydrogen bonds are formed in the open state than in the closed state of FXa. In the open state, with the larger gating distance, we detected only one hydrogen bond formed by Tyr-99-NH and Thr-95-O. In the closed state, each gating residue can form one or more hydrogen bonds with the other residues on FXa. Furthermore, each gating residue has at least one intra-molecular hydrogen bond with a lifetime higher than 10%, which is considered significant because of the transient nature of the hydrogen bond. Among the hydrogen bonds detected, the one formed by Ile-176-NH and Phe-174-O was notable for its high lifetime (91.7%). The hydrogen bond network in the closed state of FXa is believed to play a significant role in maintaining the closed conformation of the aryl-binding site.

**Table 2** Values of the hydrophobic and total solvent accessible surface areas (SASA, $nm^2$) for the open and closed systems of FXa

| Residue | Open system | | Closed system | |
|---|---|---|---|---|
| | Total SASA | HSASA[a] | Total SASA | HSASA |
| His-57 | 0.70 | 0.20 | 0.40 | 0.11 |
| Tyr-99 | 0.78 | 0.14 | 0.46 | 0.15 |
| Asp-102 | 0.57 | 0.15 | 0.37 | 0.15 |
| Phe-174 | 0.26 | 0.16 | 0.32 | 0.15 |
| Asp-189 | 1.18 | 0.12 | 1.06 | 0.13 |
| Ser-195 | 0.33 | 0.10 | 0.19 | 0.14 |
| Trp-215 | 0.03 | 0.04 | 0.03 | 0.04 |
| FXa[b] | 0.51±0.44 | 0.13±0.07 | 0.51±0.43 | 0.14±0.09 |

[a] Hydrophobic SASA

[b] Values from the entire FXa protein

**Table 3** Intramolecular hydrogen bonds formed by the gating residues in both the open and closed states of FXa

| Donor | Acceptor | Lifetime[a] (%) | | Distance[b] (nm) | |
|---|---|---|---|---|---|
| | | Open | Closed | Open | Closed |
| Tyr-99-NH | Lys-96-O | 0 | 12.6 | 1.18±0.13 | 0.51±0.12 |
| Tyr-99-NH | Thr-95-O | 34.9 | 12.0 | 0.45±0.19 | 0.47±0.12 |
| Phe-174-NH | Ser-172-Oγ | 0 | 20.1 | 0.65±0.05 | 0.53±0.14 |
| Ile-176-NH | Phe174-O | 0 | 91.7 | 0.76±0.19 | 0.31±0.03 |
| Trp-215-NH | Ser214-Oγ | 0 | 48.8 | 0.48±0.02 | 0.35±0.04 |
| Trp-215-NH | Ile-227-O | 0 | 0.33 | 0.46±0.05 | 0.51±0.06 |
| Ile-227-NH | Trp-215-O | 0 | 6.65 | 1.78±0.13 | 0.47±0.07 |

[a] Percentage of time in which the distance between a donor and an acceptor is within the defined distance of a hydrogen bond. The time resolution used to collect the statistics is 1 ps. Due to the transient nature of hydrogen bonds, a lifetime of 10% is considered "significant"; a lifetime of 50% is considered "strong"

[b] Average distance between donor and acceptor

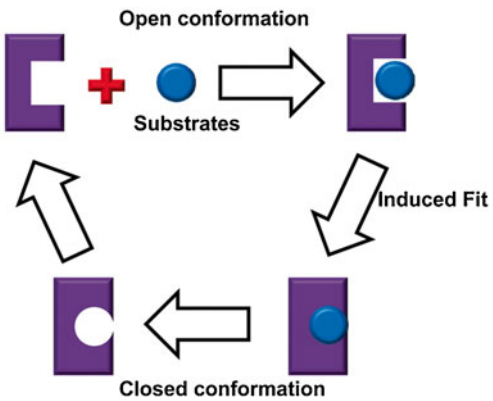


**Fig. 6** Conversion between different states of FXa. Zymogen human coagulation Factor X is converted to FXa by proteolytic cleavage. The resulting FXa combines with FVa on the membrane of platelets, and adopts the open conformation. The closed conformation is induced upon binding of a substrate. After the substrate is proteolyzed and dissolved, FXa returns to the open conformation

It is well-known that proteins have diversity in their conformations, which is an intrinsic and substantial feature of proteins. From our MD simulations, we observed "conformational diversity" in both the open and closed states of the FXa molecule. However, in contrast to the study of Singh and Briggs [16], we did not observe a directional transition from the open state to the closed state or from the closed state to the open state under our MD simulation conditions. However, our result is consistent with the "induced fit" model, in which transition from the open state (which allows the binding of substrate of variable size) to the closed state (which is fit only for a particular substrate) is induced by the presence of substrate. The discrepancy between our results and those of Singh and Briggs [16] can be explained by the different conditions applied in their study, in which an external force was introduced into their simulations.

The findings obtained in our study provide a better understanding of the enzyme–substrate interaction and the mechanism of protein conformation change involved in human coagulation Factor X. These findings could lead to new strategies in the development of novel therapeutics and drugs, especially anticoagulant and antithrombotic drugs.

## Conclusions

In the current study, 30-ns MD simulations were performed on both the open and closed states of human FXa—a critical factor in the activation and regulation of the blood coagulation cascade. By comparing MD trajectories in the open and closed states of FXa, we found conformational diversity in the aryl-binding site in both the system. However, in the open state, the aryl-binding site formed a spatial conformation with a larger gating distance, which allows substrate residues with hydrophobic side chains of variable size to enter. The open state conformation has a generally larger hydrophobic or total SASA on its surface residues, which can interact with substrates from small to large size. In contrast, the closed state of FXa, which is possibly induced by ligand binding via strong hydrogen bonds, has a smaller S4 binding pocket than that of the open state. The small S4 binding pocket is fit only for a particular substrate. We propose a mechanism that explains how human coagulation Factor X function is regulated and how its FXa interacts with its substrates (Fig. 6): zymogen human coagulation Factor X is converted to FXa by proteolytic cleavage between residues Arg-15 and Ile-16; the resulting FXa combines with FVa on the membrane of platelets in a $Ca^{2+}$-dependent association, and adopts the open conformation; upon interaction with a substrate, the closed conformation is induced, which is fit for the particular substrate only; after the substrate is proteolyzed and dissolved, FXa returns to the open conformation and is ready to interact with the next substrate molecule.

**Acknowledgments** This work was supported by the grants from the National Basic Research Program of China (973 Program, No. 2011CB910204 and 2012CB316501), Research Program of CAS (KSCX2-EW-R-04), National Natural Science Foundation of China (No. 30900272), Shanghai Natural Science Foundation (No. 10ZR1421500), China Postdoctoral Science Foundation (No. 20110490068), and in part by Shanghai Pujiang Scholarship Program (No. 10PJ1408000). The authors gratefully acknowledge the support of SA-SIBS scholarship program.

## References

1. Davie EW, Fujikawa K, Kisiel W (1991) The coagulation cascade: initiation, maintenance, and regulation. Biochemistry 30:10363–10370
2. Mann KG, Nesheim ME, Church WR, Haley P, Krishnaswamy S (1990) Surface-dependent reactions of the vitamin K-dependent enzyme complexes. Blood 76:1–16
3. Caldwell SH, Hoffman M, Lisman T, Macik BG, Northup PG, Reddy KR, Tripodi A, Sanyal AJ (2006) Coagulation disorders and hemostasis in liver disease: pathophysiology and critical assessment of current management. Hepatology 44:1039–1046
4. Kozek-Langenecker S (2007) Management of massive operative blood loss. Minerva Anestesiol 73:401–415
5. Soliman DE, Broadman LM (2006) Coagulation defects. Anesthesiol Clin 24:549–578, vii
6. Telfer TP, Denson KW, Wright DR (1956) A new coagulation defect. Br J Haematol 2:308–316
7. Graham JB, Barrow EM, Hougie C (1957) Stuart clotting defect. II. Genetic aspects of a new hemorrhagic state. J Clin Invest 36:497–503
8. Bode W, Mayr I, Baumann U, Huber R, Stone SR, Hofsteenge J (1989) The refined 1.9 A crystal structure of human alpha-thrombin: interaction with D-Phe-Pro-Arg chloromethylketone and significance of the Tyr-Pro-Pro-Trp insertion segment. EMBO J 8:3467–3475
9. Katz BA, Elrod K, Luong C, Rice MJ, Mackman RL, Sprengeler PA, Spencer J, Hataye J, Janc J, Link J, Litvak J, Rai R, Rice K, Sideris S, Verner E, Young W (2001) A novel serine protease inhibition motif involving a multi-centered short hydrogen bonding network at the active site. J Mol Biol 307:1451–1486
10. Bode W, Turk D, Karshikov A (1992) The refined 1.9-A X-ray crystal structure of D-Phe-Pro-Arg chloromethylketone-inhibited human alpha-thrombin: structure analysis, overall structure, electrostatic properties, detailed active-site geometry, and structure-function relationships. Protein Sci 1:426–471
11. Katz BA, Elrod K, Verner E, Mackman RL, Luong C, Shrader WD, Sendzik M, Spencer JR, Sprengeler PA, Kolesnikov A, Tai VW, Hui HC, Breitenbucher JG, Allen D, Janc JW (2003) Elaborate manifold of short hydrogen bond arrays mediating binding of active site-directed serine protease inhibitors. J Mol Biol 329:93–120
12. Katz BA, Mackman R, Luong C, Radika K, Martelli A, Sprengeler PA, Wang J, Chan H, Wong L (2000) Structural basis for selectivity of a small molecule, S1-binding, submicromolar inhibitor of urokinase-type plasminogen activator. Chem Biol 7:299–312
13. Katz BA, Spencer JR, Elrod K, Luong C, Mackman RL, Rice M, Sprengeler PA, Allen D, Janc J (2002) Contribution of multi-centered short hydrogen bond arrays to potency of active site-

directed serine protease inhibitors. J Am Chem Soc 124:11657–11668
14. Parker ET, Pohl J, Blackburn MN, Lollar P (1997) Subunit structure and function of porcine factor Xa-activated factor VIII. Biochemistry 36:9365–9373
15. Padmanabhan K, Padmanabhan KP, Tulinsky A, Park CH, Bode W, Huber R, Blankenship DT, Cardin AD, Kisiel W (1993) Structure of human des(1–45) factor Xa at 2.2 A resolution. J Mol Biol 232:947–966
16. Singh N, Briggs JM (2008) Molecular dynamics simulations of Factor Xa: insight into conformational transition of its binding subsites. Biopolymer 89:1104–1113
17. Wang JF, Wei DQ, Li L, Zheng SY, Li YX, Chou KC (2007) 3D structure modeling of cytochrome P450 2 C19 and its implication for personalized drug design. Biochem Biophys Res Commun 355:513–519
18. Wang JF, Wei DQ, Lin Y, Wang YH, Du HL, Li YX, Chou KC (2007) Insights from modeling the 3D structure of NAD(P)H-dependent D-xylose reductase of Pichia stipitis and its binding interactions with NAD and NADP. Biochem Biophys Res Commun 359:323–329
19. Wang JF, Wei DQ, Chen C, Li Y, Chou KC (2008) Molecular modeling of two CYP2C19 SNPs and its implications for personalized drug design. Protein Peptide Lett 15:27–32
20. Wang JF, Gong K, Wei DQ, Li YX, Chou KC (2009) Molecular dynamics studies on the interactions of PTP1B with inhibitors: from the first phosphate-binding site to the second one. Protein Eng Des Sel 22:349–355
21. Wang JF, Wei DQ, Chou KC (2009) Insights from investigating the interactions of adamantane-based drugs with the M2 proton channel from the H1N1 swine virus. Biochem Biophys Res Commun 388:413–417
22. Zeng QK, Du HL, Wang JF, Wei DQ, Wang XN, Li YX, Lin Y (2009) Reversal of coenzyme specificity and improvement of catalytic efficiency of Pichia stipitis xylose reductase by rational site-directed mutagenesis. Biotechnol Lett 31:1025–1029
23. Wang Y, Wei DQ, Wang JF (2010) Molecular dynamics studies on T1 lipase: insight into a double-flap mechanism. J Chem Inf Model 50:875–878
24. Guo X, Wang JF, Zhu Y, Wei DQ (2010) Recent progress on computer-aided inhibitor design of H5N1 influenza A virus. Curr Comput Aided Drug Des 6:139–146
25. Wang JF, Wei DQ (2009) Role of structural bioinformatics and traditional Chinese medicine databases in pharmacogenomics. Pharmacogenomics 10:1213–1215
26. Wang JF, Chou KC (2010) Molecular modeling of cytochrome P450 and drug metabolism. Curr Drug Metab 11:342–346
27. Wang JF, Chou KC (2010) Insights from studying the mutation-induced allostery in the M2 proton channel by molecular dynamics. Protein Eng Des Sel 23:663–666
28. Li L, Wei DQ, Wang JF, Chou KC (2007) Computational studies of the binding mechanism of calmodulin with chrysin. Biochem Biophys Res Commun 358:1102–1107
29. Wang JF, Wei DQ, Chou KC (2008) Drug candidates from traditional chinese medicines. Curr Top Med Chem 8:1656–1665
30. Lian P, Wei DQ, Wang JF, Chou KC (2011) An allosteric mechanism inferred from molecular dynamics simulations on phospholamban pentamer in lipid membranes. PLoS One 6: e18587
31. Wang JF, Wei DQ, Chou KC (2008) Pharmacogenomics and personalized use of drugs. Curr Top Med Chem 8:1573–1579
32. Gong K, Li L, Wang JF, Cheng F, Wei DQ, Chou KC (2009) Binding mechanism of H5N1 influenza virus neuraminidase with ligands and its implication for drug design. Med Chem 5:242–249
33. Wang JF, Chou KC (2011) Insights from modeling the 3D structure of New Delhi metallo-β-lactamse and its binding interactions with antibiotic drugs. PLoS One 6:e18414
34. Gu RX, Gu H, Xie ZY, Wang JF, Arias HR, Wei DQ, Chou KC (2009) Possible drug candidates for Alzheimer's disease deduced from studying their binding interactions with alpha7 nicotinic acetylcholine receptor. Med Chem 5:250–262
35. Wang JF, Yan JY, Wei DQ, Chou KC (2009) Binding of CYP2C9 with diverse drugs and its implications for metabolic mechanism. Med Chem 5:263–270
36. Wang JF, Zhang CC, Chou KC, Wei DQ (2009) Structure of cytochrome p450s and personalized drug. Curr Med Chem 16:232–244
37. Chen Q, Zhang T, Wang JF, Wei DQ (2011) Advances in human cytochrome P450 and personalized medicine. Curr Drug Metab 12:436–444
38. Daura X, Haaksma E, van Gunsteren WF (2000) Factor Xa: simulation studies with an eye to inhibitor design. J Comput Aided Mol Des 14:507–529
39. Venkateswarlu D, Perera L, Darden T, Pedersen LG (2002) Structure and dynamics of zymogen human blood coagulation factor X. Biophys J 82:1190–1206
40. Corte JR, Fang T, Pinto DJ, Han W, Hu Z, Jiang XJ, Li YL, Gauuan JF, Hadden M, Orton D, Rendina AR, Luettgen JM, Wong PC, He K, Morin PE, Chang CH, Cheney DL, Knabb RM, Wexler RR, Lam PY (2008) Structure-activity relationships of anthranilamide-based factor Xa inhibitors containing piperidinone and pyridinone P4 moieties. Bioorg Med Chem Lett 18:2845–2849
41. Berman HM, Westbrook J, Feng Z, Gilliland G, Bhat TN, Weissig H, Shindyalov IN, Bourne PE (2000) The protein data bank. Nucleic Acids Res 28:235–242
42. Underwood MC, Zhong D, Mathur A, Heyduk T, Bajaj SP (2000) Thermodynamic linkage between the S1 stie, the Na + site, and the Ca2+ site in the protease domain of human coagulation factor xa. J Biol Chem 275:36876–36884
43. Griffon N, Di Stasio E (2001) Thermodynamics of Na + binding to coagulation serine proteases. Biophys Chem 90:89–96
44. Van Der Spoel D, Lindahl E, Hess B, Groenhof G, Mark AE, Berendsen HJ (2005) GROMACS: fast, flexible, and free. J Comput Chem 26:1701–1718
45. Scott WRP, Hüenenberger PH, Tironi IG, Mark AE, Billeter SR, Fennen J, Torda AE, Huber T, Krueger P, van Gunsteren WF (1999) The GROMOS biomolecular simulation program package. J Phys Chem A 103:3596–3607
46. Aalten DM van, Bywater R, Findlay JB, Hendlich M, Hooft RW, Vriend G (1996) PRODRG, a program for generating molecular topologies and unique molecular descriptors from coordinates of small molecules. J Comput Aided Mol Des 10:255–262
47. Matter H, Nazaré M, Güssregen S, Will DW, Schreuder H, Bauer A, Urmann M, Ritter K, Wagner M, Wehner V (2009) Evidence for C-Cl/C-Br…pi interactions as an important contribution to protein-ligand binding affinity. Angew Chem Int Edn Engl 48:2911–2916
48. Wallnoefer HG, Fox T, Liedl KR, Tautermann CS (2010) Dispersion dominate halogen-π interactions: energies and locations of minima. Phys Chem Chem Phys 12:14941–14949
49. Sreenivasan U, Axelsen PH (1992) Buried water in homologous serine proteases. Biochemistry 31:12785–12791
50. Guvench O, Price DJ, Brooks CL III (2005) Receptor rigidity and ligand mobility in trypsin-ligand complexes. Proteins 58:407–417
51. Lesk AM, Fordham WD (1996) Conservation and variability in the structures of serine proteinases of the chymotrypsin family. J Mol Biol 258:501–537
52. Wallnoefer HG, Handschuh S, Liedl KR, Fox T (2010) Stabilizing of a globular protein by a highly complex water network: a

molecular dynamics simulation study on factor Xa. J Phys Chem B 114:7405–7412
53. Miller CA, Gellman SH, Abbott NL, de Pablo JJ (2009) Association of helical beta-peptides and their aggregation behavior from the potential of mean force in explicit solvent. Biophys J 96:4349–4362
54. Hlevnjak M, Zitkovic G, Zagrovic B (2010) Hydrophilicity matching: a potential prerequisite for the formation of protein-protein complexes in the cell. PLoS One 5:e11169
55. Lee C, Ham SJ (2011) Characterizing amyloid-beta protein misfolding from molecular dynamics simulations with explicit water. J Comput Chem 32:349–355